

Longitudinal Dynamics

6

6.1 Response to controls

The solution of the longitudinal equations of motion by, for example, the methods described in Chapter 5 enables the response transfer functions to be obtained. These completely describe the linear dynamic response to a control input in the plane of symmetry. Implicit in the response are the dynamic properties determined by the stability characteristics of the aeroplane. The transfer functions and the response variables described by them are linear, since the entire modelling process is based on the assumption that the motion is constrained to small disturbances about an equilibrium trim state. However, it is common practice to assume that the response to controls is valid when the magnitude of the response can hardly be described as “a small perturbation.” For many conventional aeroplanes the error incurred by so doing is generally acceptably small, as such aeroplanes tend to have substantially linear aerodynamic characteristics over their flight envelopes. For aeroplanes with very large flight envelopes, significant aerodynamic nonlinearity, and, or, dependence on sophisticated flight control systems, it is advisable not to use the linearised equations of motion for analysis of response other than that which can justifiably be described as being of small magnitude.

It is convenient to review the longitudinal response to elevator about a trim state in which thrust is held constant. The longitudinal state equation (4.67) may then be written as

$$\begin{bmatrix} \dot{u} \\ \dot{w} \\ \dot{q} \\ \dot{\theta} \end{bmatrix} = \begin{bmatrix} x_u & x_w & x_q & x_\theta \\ z_u & z_w & z_q & z_\theta \\ m_u & m_w & m_q & m_\theta \\ 0 & 0 & 1 & 0 \end{bmatrix} \begin{bmatrix} u \\ w \\ q \\ \theta \end{bmatrix} + \begin{bmatrix} x_\eta \\ z_\eta \\ m_\eta \\ 0 \end{bmatrix} \eta \quad (6.1)$$

The four response transfer functions obtained in the solution of [equation \(6.1\)](#) may conveniently be written as

$$\frac{u(s)}{\eta(s)} \equiv \frac{N_\eta^u(s)}{\Delta(s)} = \frac{k_u(s + 1/T_u)(s^2 + 2\zeta_u\omega_u s + \omega_u^2)}{(s^2 + 2\zeta_p\omega_p s + \omega_p^2)(s^2 + 2\zeta_s\omega_s s + \omega_s^2)} \quad (6.2)$$

$$\frac{w(s)}{\eta(s)} \equiv \frac{N_\eta^w(s)}{\Delta(s)} = \frac{k_w(s + 1/T_\alpha)(s^2 + 2\zeta_\alpha\omega_\alpha s + \omega_\alpha^2)}{(s^2 + 2\zeta_p\omega_p s + \omega_p^2)(s^2 + 2\zeta_s\omega_s s + \omega_s^2)} \quad (6.3)$$

$$\frac{q(s)}{\eta(s)} \equiv \frac{N_\eta^q(s)}{\Delta(s)} = \frac{k_qs(s + 1/T_{\theta_1})(s + 1/T_{\theta_2})}{(s^2 + 2\zeta_p\omega_p s + \omega_p^2)(s^2 + 2\zeta_s\omega_s s + \omega_s^2)} \quad (6.4)$$

$$\frac{\theta(s)}{\eta(s)} \equiv \frac{N_\eta^\theta(s)}{\Delta(s)} = \frac{k_\theta(s + 1/T_{\theta_1})(s + 1/T_{\theta_2})}{(s^2 + 2\zeta_p\omega_p s + \omega_p^2)(s^2 + 2\zeta_s\omega_s s + \omega_s^2)} \quad (6.5)$$

The solution of the equations of motion results in polynomial descriptions of the transfer function numerators and common denominator, as set out in Appendix 3. The polynomials factorise into real and complex pairs of roots, which are most explicitly quoted in the style of [equations \(6.2\) through \(6.5\)](#). Since the roots are interpreted as time constants, damping ratios, and natural frequencies, this style of writing makes the essential information instantly available. It should also be noted that the numerator and denominator factors are typical for a conventional aeroplane. Sometimes complex pairs of roots may become two real roots and vice versa. However, this does not usually mean that the dynamic response characteristics of the aeroplane become dramatically different. Differences in the interpretation of response may be evident but will not necessarily be large.

As has already been indicated, the common denominator of the transfer functions describes the characteristic polynomial, which in turn describes the stability characteristics of the aeroplane. Thus the response of all variables to an elevator input is dominated by the denominator parameters: damping ratios and natural frequencies. The differences between the individual responses are entirely determined by their respective numerators. It is therefore important to fully appreciate the role of the numerator in determining response dynamics. The *response shapes* of the individual variables are determined by the common denominator and “coloured” by their respective numerators. The numerator plays no part in determining stability in a linear system, which is how the aeroplane is modelled here.

EXAMPLE 6.1

The equations of motion and aerodynamic data for the Ling-Temco-Vought A-7A Corsair II aircraft were obtained from [Teper \(1969\)](#). The flight condition corresponds to level cruising flight at an altitude of 15,000 ft at Mach 0.3. The equations of motion, referred to a body axis system, are arranged in state space format:

$$\begin{bmatrix} \dot{u} \\ \dot{w} \\ \dot{q} \\ \dot{\theta} \end{bmatrix} = \begin{bmatrix} 0.00501 & 0.00464 & -72.90000 & -31.34000 \\ -0.08570 & -0.54500 & 309.00000 & -7.40000 \\ 0.00185 & -0.00767 & -0.39500 & 0.00132 \\ 0 & 0 & 1 & 0 \end{bmatrix} \begin{bmatrix} u \\ w \\ q \\ \theta \end{bmatrix} + \begin{bmatrix} 5.63000 \\ -23.80000 \\ -4.51576 \\ 0 \end{bmatrix} \eta \quad (6.6)$$

Since incidence α and flight path angle γ are useful variables in the evaluation of handling qualities, it is convenient to augment the corresponding output equation, as was described in Section 5.7, in order to obtain their response transfer functions in the solution of the equations of motion. The output equation is therefore

$$\begin{bmatrix} u \\ w \\ q \\ \theta \\ \alpha \\ \gamma \end{bmatrix} = \begin{bmatrix} 1 & 0 & 0 & 0 \\ 0 & 1 & 0 & 0 \\ 0 & 0 & 1 & 0 \\ 0 & 0 & 0 & 1 \\ 0 & 0.00316 & 0 & 0 \\ 0 & -0.00316 & 0 & 1 \end{bmatrix} \begin{bmatrix} u \\ w \\ q \\ \theta \\ \alpha \\ \gamma \end{bmatrix} + \begin{bmatrix} 0 \\ 0 \\ 0 \\ 0 \\ 0 \\ 0 \end{bmatrix} \eta \quad (6.7)$$

Note that all elements in the matrices in [equations \(6.6\) and \(6.7\)](#) have been rounded to five decimal places simply to keep the equations to a reasonable physical size. This should not be done with equations used in actual computation.

Solution of the equations of motion using Program CC determines the following response transfer functions:

$$\begin{aligned}
 \frac{u(s)}{\eta(s)} &= \frac{5.63(s + 0.369)(s + 0.587)(s + 58.437)}{(s^2 + 0.033s + 0.020)(s^2 + 0.902s + 2.666)} \text{ ft/s/rad} \\
 \frac{w(s)}{\eta(s)} &= \frac{-23.8(s^2 - 0.0088s + 0.0098)(s + 59.048)}{(s^2 + 0.033s + 0.020)(s^2 + 0.902s + 2.666)} \text{ ft/s/rad} \\
 \frac{q(s)}{\eta(s)} &= \frac{-4.516s(s - 0.008)(s + 0.506)}{(s^2 + 0.033s + 0.020)(s^2 + 0.902s + 2.666)} \text{ rad/s/rad (deg/s/deg)} \\
 \frac{\theta(s)}{\eta(s)} &= \frac{-4.516(s - 0.008)(s + 0.506)}{(s^2 + 0.033s + 0.020)(s^2 + 0.902s + 2.666)} \text{ rad/rad (deg/deg)} \\
 \frac{\alpha(s)}{\eta(s)} &= \frac{-0.075(s^2 - 0.0088s + 0.0098)(s + 59.048)}{(s^2 + 0.033s + 0.020)(s^2 + 0.902s + 2.666)} \text{ rad/rad (deg/deg)} \\
 \frac{\gamma(s)}{\eta(s)} &= \frac{0.075(s - 0.027)(s + 5.004)(s - 6.084)}{(s^2 + 0.033s + 0.020)(s^2 + 0.902s + 2.666)} \text{ rad/rad (deg/deg)}
 \end{aligned} \tag{6.8}$$

All coefficients have again been rounded to a convenient number of decimal places, and the previous caution should be noted.

The characteristic equation is given by equating the common denominator polynomial to zero:

$$\Delta(s) = (s^2 + 0.033s + 0.020)(s^2 + 0.902s + 2.666) = 0$$

The first pair of complex roots describes the phugoid stability mode with the following characteristics:

Damping ratio $\zeta_p = 0.11$

Undamped natural frequency $\omega_p = 0.14 \text{ rad/s}$

The second pair of complex roots describes the short-period pitching oscillation, or short-period stability mode, with the following characteristics:

Damping ratio $\zeta_s = 0.28$

Undamped natural frequency $\omega_s = 1.63 \text{ rad/s}$

These mode characteristics indicate that the airframe is aerodynamically stable, although it will be shown later that the short-period mode damping ratio is unacceptably low.

The response of the aircraft to a unit step (1°) elevator input is shown in [Fig. 6.1](#). All of the variables in the solution of the equations of motion are shown, the responses being characterised by the transfer functions, [equations \(6.8\)](#).

The responses clearly show both dynamic stability modes, the short-period pitching oscillation and the phugoid. However, the magnitude of each stability mode differs in each response

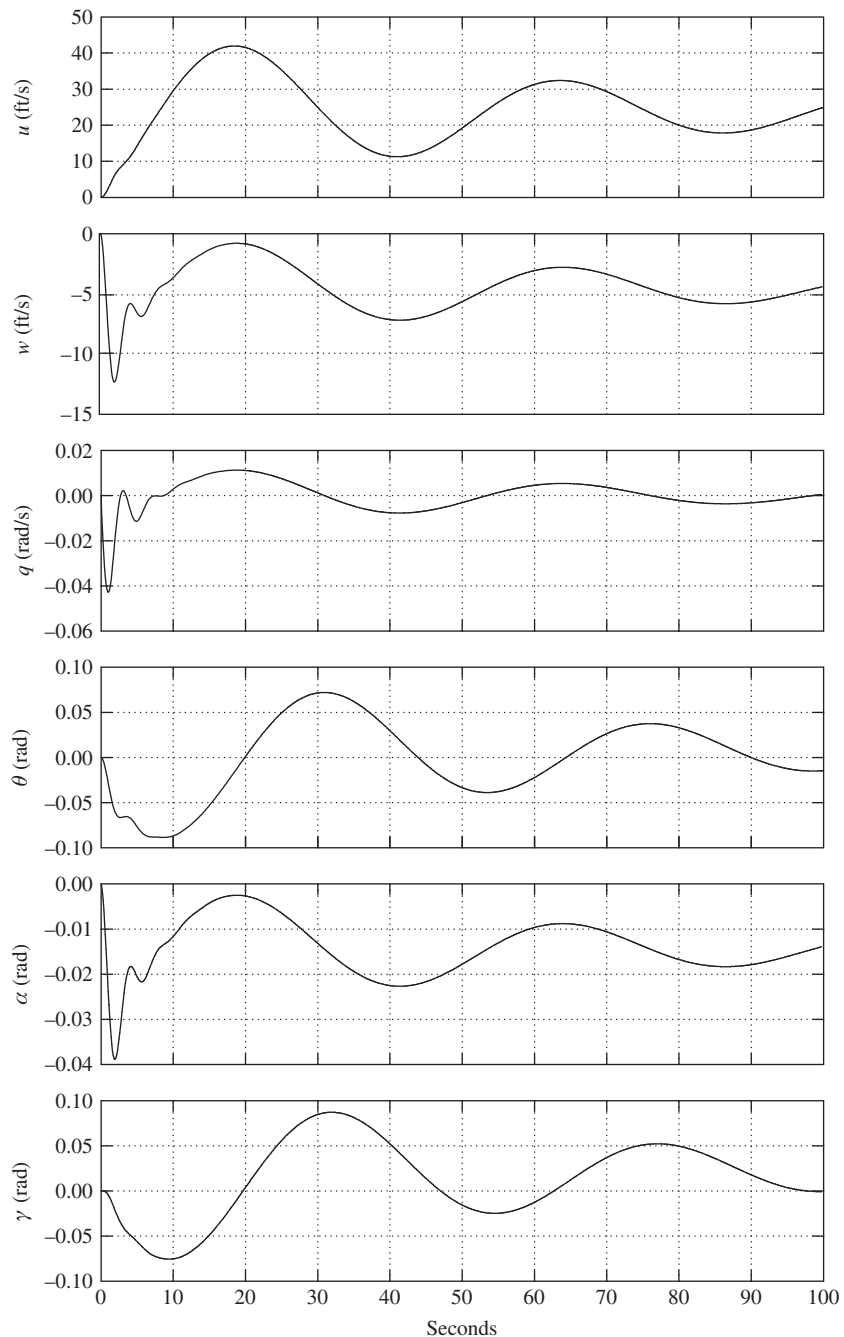


FIGURE 6.1 Aircraft response to a 1° elevator step input.

variable. For example, the short-period pitching oscillation is most visible as the initial transient in the variables w , q , and α whereas the phugoid mode is visible in all variables, although the relative magnitudes vary considerably. Clearly, the stability of the responses is the same, as determined by the common denominator of the transfer functions, [equations \(6.8\)](#), but the differences between the response variables are determined by the unique numerator of each response transfer function.

The mode content in each of the motion variables is given most precisely by the eigenvectors. The analytical procedure described in [Example 5.7](#) is applied to the equations of motion for the A-7A. With the aid of MATLAB the eigenvector matrix \mathbf{V} is determined as follows:

$$\mathbf{V} = \begin{bmatrix} & \text{short-period mode} & & \text{phugoid mode} \\ \begin{array}{cc|cc} -0.1682 - 0.1302j & -0.1682 + 0.1302j & 0.1467 + 0.9677j & 0.1467 - 0.9677j \\ 0.2993 + 0.9301j & 0.2993 - 0.9301j & 0.0410 + 0.2008j & 0.0410 - 0.2008j \\ -0.0046 + 0.0018j & -0.0046 - 0.0018j & 0.0001 + 0.0006j & 0.0001 - 0.0006j \\ 0.0019 + 0.0024j & 0.0019 - 0.0024j & 0.0041 - 0.0013j & 0.0041 + 0.0013j \end{array} \end{bmatrix} : \begin{array}{l} u \\ w \\ q \\ \theta \end{array} \quad (6.9)$$

To facilitate interpretation of the eigenvector matrix, the magnitude of each component eigenvector is calculated as follows:

$$\begin{bmatrix} 0.213 & 0.213 & 0.979 & 0.979 \\ 0.977 & 0.977 & 0.204 & 0.204 \\ 0.0049 & 0.0049 & 0.0006 & 0.0006 \\ 0.0036 & 0.0036 & 0.0043 & 0.0043 \end{bmatrix} : \begin{array}{l} u \\ w \\ q \\ \theta \end{array}$$

The phugoid mode is clearly dominant in u since $0.979 \gg 0.213$; the short-period mode is dominant in w since $0.977 \gg 0.204$; the short-period mode is dominant in q since $0.0049 \gg 0.0006$; and the contents of the short-period and phugoid modes in θ are of similar order. These observations accord very well with the responses shown in [Fig. 6.1](#).

The steady-state values of the variables following a unit step (1°) elevator input may be determined by application of the final value theorem, [equation \(5.33\)](#). The transfer functions, [equations \(6.8\)](#), assume a unit elevator displacement to mean 1 rad, and this has transfer function

$$\eta(s) = \frac{1}{s} \text{rad}$$

For a unit step input of 1° the transfer function becomes

$$\eta(s) = \frac{1}{57.3s} = \frac{0.0175}{s} \text{rad}$$

Thus, for example, the Laplace transform of the speed response to a 1° elevator step input is given by

$$u(s) = \frac{5.63(s + 0.369)(s + 0.587)(s + 58.437)}{(s^2 + 0.033s + 0.020)(s^2 + 0.902s + 2.666)} \frac{0.0175}{s} \text{ ft/s}$$

Applying the final value theorem, equation (5.33),

$$u(t)|_{ss} = \lim_{s \rightarrow 0} \left(s \frac{5.63(s + 0.369)(s + 0.587)(s + 58.437)}{(s^2 + 0.033s + 0.020)(s^2 + 0.902s + 2.666)} \frac{0.0175}{s} \right) \text{ ft/s} = 23.39 \text{ ft/s}$$

Since the step input is positive in the nose-down sense, the response eventually settles to the small steady increase in speed indicated.

In a similar way the steady-state response of all the motion variables may be calculated to give

$$\begin{bmatrix} u \\ w \\ q \\ \theta \\ \alpha \\ \gamma \end{bmatrix}_{\text{steady state}} = \begin{bmatrix} 23.39 \text{ ft/s} \\ -4.53 \text{ ft/s} \\ 0 \\ 0.34^\circ \\ -0.81^\circ \\ 1.15^\circ \end{bmatrix} \quad (6.10)$$

It is important to remember that the steady-state values given in [equation \(6.10\)](#) represent the *changes* with respect to the initial equilibrium trim state following the 1° elevator step input. Although the initial response is applied in the nose-down sense, inspection of [equation \(6.10\)](#) indicates that after the mode transients have damped out, the aircraft is left with a small reduction in incidence and a small increase in pitch attitude, and is climbing steadily at a flight path angle of 1.15° . This apparent anomaly is due to the fact that at the chosen flight condition the aircraft is operating close to the stall boundary on the *back side* of the drag speed curve—that is, below the minimum drag speed. Thus the disturbance results in a significant decrease in drag, leaving the aircraft with sufficient excess power to climb gently. It is for the same reason that a number of the transfer functions, [equations \(6.8\)](#), have non-minimum phase numerator terms where these would not normally be expected.

6.1.1 The characteristic equation

The longitudinal characteristic polynomial for a classical aeroplane is fourth order; it determines the common denominator in the longitudinal response transfer functions and, when equated to zero, defines the characteristic equation, which may be written as

$$As^4 + Bs^3 + Cs^2 + Ds + E = 0 \quad (6.11)$$

The characteristic [equation \(6.11\)](#) most commonly factorises into two pairs of complex roots, which are most conveniently written as

$$(s^2 + 2\zeta_p\omega_ps + \omega_p^2)(s^2 + 2\zeta_s\omega_ss + \omega_s^2) = 0 \quad (6.12)$$

As already explained, the second-order characteristics in [equation \(6.12\)](#) describe the phugoid and short-period stability modes, respectively. The stability modes that make up [equation \(6.12\)](#) provide a *complete description* of the longitudinal stability properties of the aeroplane subject to the constraint of small-perturbation motion. Interpretation of the characteristic equation written in

this way is most readily accomplished if reference is first made to the properties of the classical mechanical mass-spring-damper system, which are summarised in Appendix 6.

Thus the longitudinal dynamics of the aeroplane may be likened to a pair of loosely coupled mass-spring-damper systems, and the interpretation of the motion of the aeroplane following a disturbance from equilibrium may be made by direct comparison with the behaviour of the mechanical mass-spring-damper. However, the damping and frequency characteristics of the aeroplane are obviously not mechanical in origin; they derive entirely from the aerodynamic properties of the airframe. The connection between the observed dynamics of the aeroplane and its aerodynamic characteristics is made by comparing [equation \(6.12\)](#) with [equation \(6.11\)](#) and then referring to Appendix 3 for the definitions of the coefficients in [equation \(6.11\)](#) in terms of aerodynamic stability derivatives. Clearly, the relationships between the damping ratios and the undamped frequencies of [equation \(6.12\)](#), and their aerodynamic *drivers*, are neither obvious nor simple. Means for dealing with this difficulty are described in the following sections; simplifying approximations are made based on the observation and understanding of the physical behaviour of aeroplane dynamics.

6.2 The dynamic stability modes

Both longitudinal dynamic stability modes are excited whenever the aeroplane is disturbed from its equilibrium trim state. A disturbance may be initiated by pilot control inputs, by a change in power setting, by airframe configuration changes, such as flap deployment, and by external atmospheric influences such as gusts and turbulence.

6.2.1 The short-period pitching oscillation

The short-period mode is typically a damped oscillation in pitch about the oy axis. Whenever an aircraft is disturbed from its pitch equilibrium state, the mode is excited and manifests itself as a classical second-order oscillation in which the principal variables are incidence $\alpha(w)$, pitch rate q , and pitch attitude θ . This observation is easily confirmed by reference to the eigenvectors in the solution of the equations of motion; it may be seen in Example 6.1 and in [Fig. 6.1](#). Typically, the undamped natural frequency of the mode is in the range 1 rad/s to 10 rad/s, and the damping is usually stabilizing, although the damping ratio is often lower than desired. A significant feature of the mode is that the speed remains approximately constant ($u = 0$) during a disturbance. As the period of the mode is short, inertia and momentum effects ensure that speed response in the time scale of the mode is negligible.

The physical situation applying can be interpreted by comparison with a torsional mass-spring-damper system. The aircraft behaves as if it were restrained by a torsional spring about the oy axis, as indicated in [Fig. 6.2](#). A pitch disturbance from trim equilibrium causes the “spring” to produce a restoring moment, thereby giving rise to an oscillation in pitch. The oscillation is damped and this can be interpreted as a viscous damper as suggested in [Fig. 6.2](#). Of course, the spring and viscous damping effects are not mechanical. In reality, they are produced entirely by aerodynamic mechanisms with contributions from all parts of the airframe, not all of which are necessarily stabilising. However, in the interests of promoting understanding, the stiffness and damping effects are assumed to be dominated by the aerodynamics of the tailplane. The spring stiffness arises from the

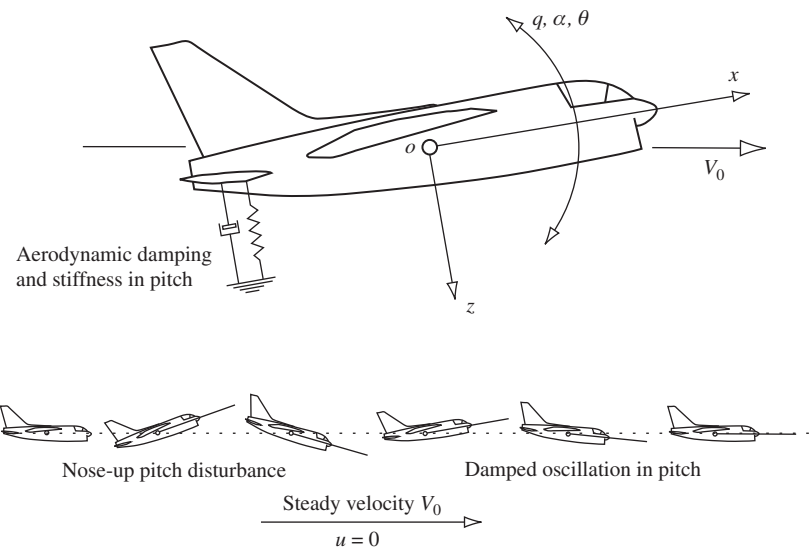


FIGURE 6.2 Stable short-period pitching oscillation.

natural *weathercock* tendency of the tailplane to align with the incident flow. The damping arises from the motion of the tailplane during the oscillation when, clearly, it behaves as a kind of viscous paddle damper. The total observed mode dynamics depend not only on the tailplane contribution but also on the magnitudes of the additional contributions from other parts of the airframe. When the overall stability is marginal, it is implied that the additional contributions are significant, which makes it much more difficult to identify and quantify the principal aerodynamic mode drivers.

6.2.2 The phugoid

The phugoid mode is most commonly a lightly damped low-frequency oscillation in speed u , which couples into pitch attitude θ and height h . A significant feature of this mode is that the incidence $\alpha(w)$ remains substantially constant during a disturbance. Again, these observations are easily confirmed by reference to the eigenvectors in the solution of the equations of motion, which may be seen in Example 6.1 and in Fig. 6.1. However, it is clear that the phugoid appears, to a greater or lesser extent, in all of the longitudinal motion variables; however, the relative magnitudes of the phugoid components in incidence $\alpha(w)$ and in pitch rate q are very small. Typically, the undamped natural frequency of the phugoid is in the range 0.1 rad/s to 1 rad/s and the damping ratio is very low. However, the apparent damping characteristics of the mode may be substantially influenced by power effects in some aeroplanes.

Consider the development of classical phugoid motion following a small disturbance in speed, as illustrated in Fig. 6.3. Initially the aeroplane is in trimmed level equilibrium flight with steady velocity V_0 such that lift L and weight mg are equal. Let the aeroplane be disturbed (Fig 6.3a) such

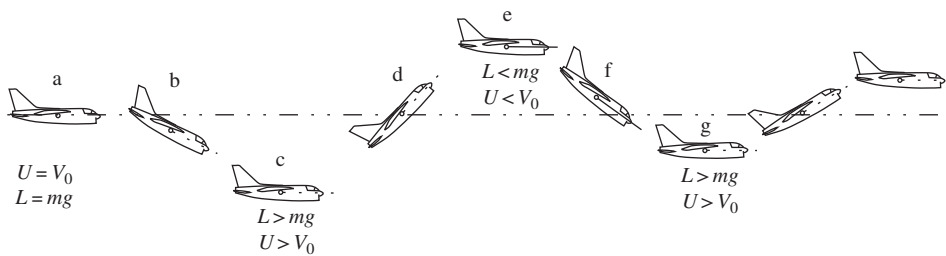


FIGURE 6.3 Development of a stable phugoid.

that the velocity is reduced by a small amount u . Since the incidence remains substantially constant, this results in a small reduction in lift such that the aeroplane is no longer in vertical equilibrium. It therefore starts to lose height and, since it is flying “downhill,” starts to accelerate (Fig. 6.3b). The speed continues to build up to a value in excess of V_0 , which is accompanied by a build up in lift which eventually exceeds the weight by a significant margin. The build up in speed and lift causes the aircraft to pitch up steadily until it starts to climb (Fig. 6.3c). Since it now has an excess of kinetic energy, inertia and momentum effects cause it to fly up through the nominal trimmed height datum (Fig. 6.3d), losing speed and lift as it goes because it is now flying “uphill.” As it decelerates it pitches down steadily until its lift is significantly less than the weight and the accelerating descent starts again (Fig. 6.3e). Inertia and momentum effects cause the aeroplane to continue flying down through the nominal trimmed height datum (Fig. 6.3f), and, as speed and lift continue to build up, it pitches up steadily until it starts climbing again to commence the next cycle of oscillation (Fig. 6.3g). As the motion progresses the effects of drag cause the motion variable maxima and minima at each peak to reduce gradually in magnitude until the motion eventually damps out.

Thus the phugoid is classical damped harmonic motion resulting in the aircraft flying a gentle sinusoidal flight path about the nominal trimmed height datum. As large inertia and momentum effects are involved, the motion is necessarily relatively slow such that the angular accelerations, \dot{q} and $\dot{\alpha}(w)$, are insignificantly small. Consequently, the natural frequency of the mode is low and, since drag is designed to be low, the damping is also low. Typically, once excited, many cycles of the phugoid may be visible before it eventually damps out. Since the rate of energy loss is low, a consequence of low drag damping effects, the motion is often approximated by undamped harmonic motion, in which potential and kinetic energy are exchanged as the aircraft flies the sinusoidal flight path. This in fact was the basis on which [Lanchester \(1908\)](#) first successfully analysed the motion.

6.3 Reduced-order models

Thus far the emphasis has been on the exact solution of the longitudinal equations of motion which results in an exact description of the stability and response characteristics of the aircraft. Although this is usually the object of a flight dynamics investigation, it has two disadvantages. First, a computational facility is required if a very tedious manual solution is to be avoided; second, it is

difficult, if not impossible, to establish the relationships between the stability characteristics and their aerodynamic drivers. Both of these disadvantages can be avoided by seeking approximate solutions, which can also provide considerable insight into the physical phenomena governing the dynamic behaviour of the aircraft.

For example, an approximate solution of the longitudinal characteristic [equation, \(6.11\)](#), is based on the fact that the coefficients A , B , C , D , and E have relative values which do not change very much for conventional aeroplanes. Generally A , B , and C are significantly larger than D and E such that the quartic has the following approximate factors:

$$A \left(s^2 + \frac{(CD - BE)}{C^2} s + \frac{E}{C} \right) \left(s^2 + \frac{B}{A} s + \frac{C}{A} \right) = 0 \quad (6.13)$$

[Equation \(6.13\)](#) is in fact the first step in the classical manual iterative solution of the quartic; the first pair of complex roots describes the phugoid mode, and the second pair describes the short-period mode. Algebraic expressions, in terms of aerodynamic derivatives, mass and inertia parameters, etc. for the coefficients A , B , C , D , and E are given in [Appendix 3](#). Since these expressions are relatively complex, further physical insight is not particularly revealing unless simplifying assumptions are made. However, the approximate solution given by [equation \(6.13\)](#) is often useful for preliminary mode evaluations, or as a check of computer solutions, when the numerical values of the coefficients A , B , C , D , and E are known. For conventional aeroplanes the approximate solution is often surprisingly close to the exact solution of the characteristic equation.

6.3.1 The short-period mode approximation

The short-term response characteristics of an aircraft are of particular importance in consideration of flying and handling qualities for the reasons discussed in [Section 6.5](#). Since short-term behaviour is dominated by the short-period mode, it is convenient to obtain the *reduced-order* equations of motion in which the phugoid is suppressed or omitted. By observing the nature of the short-period pitching oscillation, sometimes called *rapid incidence adjustment*, it is possible to simplify the longitudinal equations of motion to describe short-term dynamics only. The terms remaining in the reduced-order equations of motion are therefore the terms which dominate short-term dynamics, thereby providing insight into the important aerodynamic drivers governing physical behaviour.

It has already been established that the short-period pitching oscillation is almost exclusively an oscillation in which the principal variables are pitch rate q and incidence α , with the speed remaining essentially constant; thus $u = 0$. Therefore, the speed equation and the speed-dependent terms may be removed from the longitudinal equations of motion, (6.1); since they are all approximately zero in short-term motion, the revised equations may be written as

$$\begin{bmatrix} \dot{w} \\ \dot{q} \\ \dot{\theta} \end{bmatrix} = \begin{bmatrix} z_w & z_q & z_\theta \\ m_w & m_q & m_\theta \\ 0 & 1 & 0 \end{bmatrix} \begin{bmatrix} w \\ q \\ \theta \end{bmatrix} + \begin{bmatrix} z_\eta \\ m_\eta \\ 0 \end{bmatrix} \eta \quad (6.14)$$

Further, assuming that the equations of motion are referred to aircraft wind axes and that the aircraft is initially in steady level flight, then

$$\theta_e \equiv \alpha_e = 0 \quad \text{and} \quad U_e = V_0$$

and, with reference to Appendix 2, it follows that

$$z_\theta = m_\theta = 0$$

Equation (6.14) then reduces to its simplest possible form:

$$\begin{bmatrix} \dot{w} \\ \dot{q} \end{bmatrix} = \begin{bmatrix} z_w & z_q \\ m_w & m_q \end{bmatrix} \begin{bmatrix} w \\ q \end{bmatrix} + \begin{bmatrix} z_\eta \\ m_\eta \end{bmatrix} \eta \quad (6.15)$$

where now the derivatives are referred to a wind axes system. Equation (6.15) is sufficiently simple that the transfer function matrix may be calculated manually by the application of equation (5.53):

$$\mathbf{G}(s) = \frac{\mathbf{N}(s)}{\Delta(s)} = \frac{\begin{bmatrix} s - m_q & z_q \\ m_w & s - z_w \end{bmatrix} \begin{bmatrix} z_\eta \\ m_\eta \end{bmatrix}}{\begin{vmatrix} s - z_w & -z_q \\ -m_w & s - m_q \end{vmatrix}} = \frac{\begin{bmatrix} z_\eta \left(s + \left(m_q + z_w \frac{m_\eta}{z_\eta} \right) \right) \\ m_\eta \left(s + \left(m_w \frac{z_\eta}{m_\eta} - z_w \right) \right) \end{bmatrix}}{(s^2 - (m_q + z_w)s + (m_q z_w - m_w z_q))} \quad (6.16)$$

The transfer functions may be further simplified by noting that

$$z_q \frac{m_\eta}{z_\eta} > > m_q \quad \text{and} \quad -z_w > > m_w \frac{z_\eta}{m_\eta}$$

and, with reference to Appendix 2,

$$z_q = \frac{\overset{\circ}{Z}_q + mU_e}{m - \overset{\circ}{Z}_{\dot{w}}} \cong U_e$$

since

$$\overset{\circ}{Z}_q < < mU_e \quad \text{and} \quad m > > \overset{\circ}{Z}_{\dot{w}}$$

Thus the two short-term transfer functions describing response to elevator may be written as

$$\frac{w(s)}{\eta(s)} = \frac{z_\eta \left(s + U_e \frac{m_\eta}{z_\eta} \right)}{(s^2 - (m_q + z_w)s + (m_q z_w - m_w U_e))} \equiv \frac{k_w (s + 1/T_\alpha)}{(s^2 + 2\zeta_s \omega_s s + \omega_s^2)} \quad (6.17)$$

$$\frac{q(s)}{\eta(s)} = \frac{m_\eta (s - z_w)}{(s^2 - (m_q + z_w)s + (m_q z_w - m_w U_e))} \equiv \frac{k_q (s + 1/T_{\theta_2})}{(s^2 + 2\zeta_s \omega_s s + \omega_s^2)} \quad (6.18)$$

where now it is understood that $k_w, k_q, T_\alpha, T_{\theta_2}, \zeta_s$, and ω_s represent approximate values. Clearly, it is now very much easier to relate the most important parameters describing the aircraft's longitudinal short-term transient dynamics to the aerodynamic properties of the airframe, represented in equations (6.17) and (6.18) by the concise derivatives.

The reduced-order characteristic equation may be written on inspection of [equation \(6.17\)](#) or [\(6.18\)](#) as

$$\Delta(s) = s^2 + 2\zeta_s \omega_s s + \omega_s^2 = s^2 - (m_q + z_w)s + (m_q z_w - m_w U_e) = 0 \quad (6.19)$$

and, by analogy with the classical mass-spring-damper system described in Appendix 6, the damping and natural frequency of the short-period mode are given, to a good approximation, by

$$\begin{aligned} 2\zeta_s \omega_s &= -(m_q + z_w) \\ \omega_s &= \sqrt{m_q z_w - m_w U_e} \end{aligned} \quad (6.20)$$

It is instructive to write the damping and natural frequency expressions (6.20) in terms of the dimensional derivatives. The appropriate conversions are obtained from Appendix 2, and the assumptions made previously are applied to give

$$\begin{aligned} 2\zeta_s \omega_s &= -\left(\frac{\dot{M}_q}{I_y} + \frac{\dot{Z}_w}{m} + \frac{\dot{M}_w U_e}{I_y}\right) \\ \omega_s &= \sqrt{\frac{\dot{M}_q \dot{Z}_w}{I_y m} - \frac{\dot{M}_w \dot{U}_e}{I_y}} \end{aligned} \quad (6.21)$$

Note that the terms on the right-hand side of expressions (6.21) comprise aerodynamic derivatives divided either by mass or by moment of inertia in pitch. These terms may be interpreted in exactly the same way as those of the classical mass-spring-damper, so it becomes apparent that the aerodynamic derivatives are providing stiffness and viscous damping in pitch, although there is more than one term contributing to damping and to natural frequency. Therefore, the aerodynamic origins of the short-period dynamics are a little more complex than those of the classical mass-spring-damper, and the various contributions do not always act in the most advantageous way. However, for conventional aeroplanes the overall dynamic characteristics usually describe a stable short-period mode.

For a typical conventional aeroplane, the relative magnitudes of the aerodynamic derivatives are such that, to a crude approximation,

$$\begin{aligned} 2\zeta_s \omega_s &= \frac{-\dot{M}_q}{I_y} \\ \omega_s &= \sqrt{\frac{-\dot{M}_w \dot{U}_e}{I_y}} \end{aligned} \quad (6.22)$$

which serves only to indicate what are usually regarded as the dominant terms governing the short-period mode. Normally, the derivative \dot{Z}_w , which is dependent on the lift curve slope of the wing, and the derivative \dot{M}_q , which is determined largely by the viscous “paddle” damping properties of the tailplane, are both negative numbers. The derivative \dot{M}_w is a measure of the aerodynamic stiffness in pitch and is also dominated by the aerodynamics of the tailplane. The sign of \dot{M}_w depends on the position of the *cg*, becoming increasingly negative as the *cg* moves forward in the airframe. Thus the short-period mode is stable if the *cg* is far enough forward in the airframe. The *cg* position

in the airframe where \dot{M}_w changes sign is called the *controls-fixed neutral point*; \dot{M}_w is therefore also a measure of the *controls-fixed stability margin* of the aircraft. With reference to [equation \(6.19\)](#) and expressions (6.20), the corresponding *cg* position where $(m_q z_w - m_w U_e)$ changes sign is called the *controls-fixed manoeuvre point* and $(m_q z_w - m_w U_e)$ is a measure of the *controls-fixed manoeuvre margin* of the aircraft. The subject of manoeuvrability is discussed in Chapter 8.

6.3.2 The phugoid mode approximation

A reduced-order model of the aircraft retaining only the phugoid dynamics is very rarely required in flight dynamics studies. However, the greatest usefulness of such a model is to identify the aerodynamic properties of the airframe that govern the characteristics of the mode.

The Lanchester model

Probably the first successful analysis of aeroplane dynamics was carried out by [Lanchester \(1908\)](#), who devised a mathematical model to describe phugoid motion based on his observations of the behaviour of gliding model aeroplanes. His analysis gives an excellent insight into the physical nature of the mode and may be applied to modern aeroplanes by interpreting and restating his original assumptions as follows:

- The aircraft is initially in steady level flight.
- The total energy of the aircraft remains constant.
- The incidence α remains constant at its initial trim value.
- The thrust τ balances the drag D .
- The motion is sufficiently slow that pitch rate q effects may be ignored.

Referring to [Fig. 6.4](#), the aircraft is initially in trimmed straight level flight with velocity V_0 . Following a disturbance in speed which excites the phugoid mode, the disturbed speed, pitch

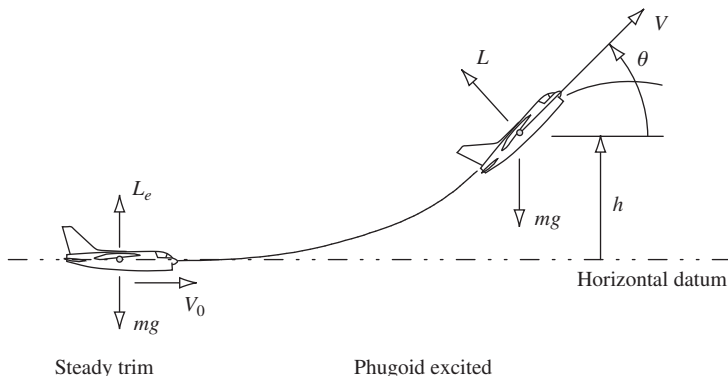


FIGURE 6.4 Phugoid oscillation.

attitude, and height are denoted V , θ , and h , respectively. Then, based on Lanchester's second assumption,

$$\frac{1}{2}mV_0^2 = \frac{1}{2}mV^2 + mgh = \text{constant}$$

whence

$$V^2 = V_0^2 - 2gh \quad (6.23)$$

which describes the exchange of kinetic and potential energy as the aeroplane flies the sinusoidal flight path.

In the initial steady trim state, the lift and weight are in balance; thus

$$L_e = \frac{1}{2}\rho V_0^2 SC_L = mg \quad (6.24)$$

and in disturbed flight the lift is given by

$$L = \frac{1}{2}\rho V^2 SC_L \quad (6.25)$$

As a consequence of Lanchester's third assumption, the lift coefficient C_L also remains constant and [equations \(6.23\), \(6.24\), and \(6.25\)](#) may be combined to give

$$L = mg - \rho gh SC_L \quad (6.26)$$

Since simple undamped oscillatory motion is assumed as a consequence of Lanchester's second assumption, the single degree of freedom equation of motion in height may be written as

$$\ddot{m}h = L \cos \theta - mg \cong L - mg \quad (6.27)$$

since, by definition, θ is a small angle. Substituting for lift L from [equation \(6.26\)](#) into [equation \(6.27\)](#),

$$\ddot{h} + \left(\frac{\rho g SC_L}{m} \right) h = \ddot{h} + \omega_p^2 h = 0 \quad (6.28)$$

Thus the frequency of the phugoid mode is given approximately by

$$\omega_p = \sqrt{\frac{\rho g SC_L}{m}} = \frac{g\sqrt{2}}{V_0} \quad (6.29)$$

when [equation \(6.24\)](#) is used to eliminate the mass.

To a reasonable approximation, then, Lanchester's model shows that the phugoid frequency is inversely proportional to the steady trimmed speed about which the mode oscillates and that its damping is zero.

A reduced-order model

A more detailed approximate model of the phugoid mode may be derived from the equations of motion by making simplifications based on assumptions about the nature of the motion. Following

a disturbance, the variables $w(\alpha)$ and q respond in the time scale associated with the short-period mode; thus it is reasonable to assume that $w(\alpha)$ and q are quasi-steady in the longer time scale associated with the phugoid. It follows that

$$\dot{w} = \dot{q} = 0$$

Once again, it is assumed that the equations of motion are referred to aircraft wind axes and, since the disturbance takes place about steady level flight,

$$\theta_e \equiv \alpha_e = 0 \quad \text{and} \quad U_e = V_0$$

With reference to Appendix 2, it follows that

$$x_\theta = -g \quad \text{and} \quad z_\theta = m_\theta = 0$$

As for the reduced-order short-period model and with reference to Appendix 2,

$$z_q = \frac{\overset{\circ}{Z}_q + mU_e}{m - \overset{\circ}{Z}_{\dot{w}}} \cong U_e$$

since

$$\overset{\circ}{Z}_q < < mU_e \quad \text{and} \quad m > > \overset{\circ}{Z}_{\dot{w}}$$

Additionally, it is usually assumed that the aerodynamic derivative x_q is insignificantly small. Thus the equations of motion (6.1) may be simplified accordingly:

$$\begin{bmatrix} \dot{u} \\ 0 \\ 0 \\ \dot{\theta} \end{bmatrix} = \begin{bmatrix} x_u & x_w & 0 & -g \\ z_u & z_w & U_e & 0 \\ m_u & m_w & m_q & 0 \\ 0 & 0 & 1 & 0 \end{bmatrix} \begin{bmatrix} u \\ w \\ q \\ \theta \end{bmatrix} + \begin{bmatrix} x_\eta \\ z_\eta \\ m_\eta \\ 0 \end{bmatrix} \eta \quad (6.30)$$

The second and third rows of equation (6.30) may be written as

$$\begin{aligned} z_u u + z_w w + U_e q + z_\eta \eta &= 0 \\ m_u u + m_w w + m_q q + m_\eta \eta &= 0 \end{aligned} \quad (6.31)$$

Equations (6.31) may be solved algebraically to obtain expressions for w and q in terms of u and η :

$$\begin{aligned} w &= \left(\frac{m_u U_e - m_q z_u}{m_q z_w - m_w U_e} \right) u + \left(\frac{m_\eta U_e - m_q z_\eta}{m_q z_w - m_w U_e} \right) \eta \\ q &= \left(\frac{m_w z_u - m_u z_w}{m_q z_w - m_w U_e} \right) u + \left(\frac{m_w z_\eta - m_\eta z_w}{m_q z_w - m_w U_e} \right) \eta \end{aligned} \quad (6.32)$$

The expressions for w and q are substituted into rows 1 and 4 of equation (6.30) and after some rearrangement, the reduced-order state equation is obtained:

$$\begin{bmatrix} \dot{u} \\ \dot{\theta} \end{bmatrix} = \begin{bmatrix} x_u - x_w \left(\frac{m_u U_e - m_q z_u}{m_w U_e - m_q z_w} \right) & -g \\ \left(\frac{m_u z_w - m_w z_u}{m_w U_e - m_q z_w} \right) & 0 \end{bmatrix} \begin{bmatrix} u \\ \theta \end{bmatrix} + \begin{bmatrix} x_\eta - x_w \left(\frac{m_\eta U_e - m_q z_\eta}{m_w U_e - m_q z_w} \right) \\ \left(\frac{m_\eta z_w - m_w z_\eta}{m_w U_e - m_q z_w} \right) \end{bmatrix} \eta \quad (6.33)$$

or

$$\dot{\mathbf{x}} = \mathbf{A}_p \mathbf{x} + \mathbf{B}_p \mathbf{u} \quad (6.34)$$

Equation (6.33) may be solved algebraically to obtain the response transfer functions for the phugoid variables u and θ . However, it is not very meaningful to analyse long-term dynamic response to elevator in this way. The characteristic equation describing the reduced-order phugoid dynamics is considerably more useful and is given by

$$\Delta(s) = \det[s\mathbf{I} - \mathbf{A}_p] = 0$$

whence

$$\begin{aligned} \Delta(s) &= s^2 + 2\zeta_p \omega_p s + \omega_p^2 \\ &= s^2 - \left(x_u - x_w \left(\frac{m_u U_e - m_q z_u}{m_w U_e - m_q z_w} \right) \right) s + g \left(\frac{m_u z_w - m_w z_u}{m_w U_e - m_q z_w} \right) \end{aligned} \quad (6.35)$$

Thus the approximate damping and natural frequency of the phugoid mode are given in terms of a limited number of aerodynamic derivatives. More explicit, but rather more approximate, insight into the aerodynamic properties of the aeroplane that dominate the mode characteristics may be obtained by making some further assumptions. Typically, for conventional aeroplanes in subsonic flight,

$$m_u \rightarrow 0, \quad |m_u z_w| << |m_w z_u| \quad \text{and} \quad |m_w U_e| >> |m_q z_w|$$

then the corresponding expressions for the damping and natural frequency become

$$\begin{aligned} 2\zeta_p \omega_p &= -x_u \\ \omega_p &= \sqrt{\frac{-g z_u}{U_e}} \end{aligned} \quad (6.36)$$

Now, with reference to Appendix 2,

$$x_u \underset{\text{def}}{\cong} \frac{\overset{\circ}{X_u}}{m} = \frac{\rho V_0 S X_u}{2m} \quad \text{and} \quad z_u \underset{\text{def}}{\cong} \frac{\overset{\circ}{Z_u}}{m} = \frac{\rho V_0 S Z_u}{2m} \quad (6.37)$$

since $\overset{\circ}{X_w}$ is negligibly small and $m > > \overset{\circ}{Z_w}$. Expressions for the dimensionless aerodynamic derivatives are given in Appendix 8 and may be approximated as shown in expressions (6.38) when the

basic aerodynamic properties are assumed to be independent of speed. This follows from the assumption that the prevailing flight condition is subsonic such that the aerodynamic properties of the airframe are not influenced by compressibility effects:

$$\begin{aligned} X_u &= -2C_D - V_0 \frac{\partial C_D}{\partial V} + \left(\frac{1}{\frac{1}{2}\rho V_0 S} \right) \frac{\partial \tau}{\partial V} \cong -2C_D \\ Z_u &= -2C_L - V_0 \frac{\partial C_L}{\partial V} \cong -2C_L \end{aligned} \quad (6.38)$$

Expressions (6.36) may therefore be restated in terms of aerodynamic parameters, assuming again that the trimmed lift is equal to the aircraft weight:

$$\begin{aligned} \zeta_p \omega_p &= \frac{g C_D}{C_L V_0} \\ \omega_p &= \sqrt{\frac{2g^2}{U_e V_0}} \equiv \frac{g\sqrt{2}}{V_0} \end{aligned} \quad (6.39)$$

A simplified approximate expression for the damping ratio follows:

$$\zeta_p \cong \frac{1}{\sqrt{2}} \left(\frac{C_D}{C_L} \right) \quad (6.40)$$

The expressions for damping ratio and natural frequency of the phugoid mode are obviously very approximate because they are the result of many simplifying assumptions. Note that the expression for ω_p is the same as that derived by Lanchester, [equation \(6.29\)](#), which indicates that the natural frequency of the phugoid mode is approximately inversely proportional to the trimmed speed. It is also interesting and important to note that the damping ratio of the phugoid mode is approximately inversely proportional to the *lift-to-drag ratio* of the aeroplane, [equation \(6.40\)](#). Since one of the main objectives of aeroplane design is to achieve a high lift-to-drag ratio it is easy to see why the damping of the phugoid mode is usually very low.

EXAMPLE 6.2

To illustrate the use of reduced-order models, consider the A-7A Corsair II aircraft of Example 6.1, at the same flight condition as in that example. Now the equations of motion in Example 6.1 are referred to a body axis system, and the use of the reduced-order models described previously requires the equations of motion referred to a wind, or stability, axis system. Using the axis transformation relationships given in Appendices 9 and 10, the stability and control derivatives and

inertia parameters referred to wind axes were calculated from the original values, which of course refer to body axes. The longitudinal state equation was then recalculated to give

$$\begin{bmatrix} \dot{u} \\ \dot{w} \\ \dot{q} \\ \dot{\theta} \end{bmatrix} = \begin{bmatrix} -0.04225 & -0.11421 & 0 & -32.2 \\ -0.20455 & -0.49774 & 317.48 & 0 \\ 0.00003 & -0.00790 & -0.39499 & 0 \\ 0 & 0 & 1 & 0 \end{bmatrix} \begin{bmatrix} u \\ w \\ q \\ \theta \end{bmatrix} + \begin{bmatrix} 0.00381 \\ -24.4568 \\ -4.51576 \\ 0 \end{bmatrix} \eta \quad (6.41)$$

The reduced-order model corresponding to the short-period approximation, as given by [equation \(6.15\)](#), is simply taken out of [equation \(6.41\)](#) and written as

$$\begin{bmatrix} \dot{w} \\ \dot{q} \end{bmatrix} = \begin{bmatrix} -0.49774 & 317.48 \\ -0.00790 & -0.39499 \end{bmatrix} \begin{bmatrix} w \\ q \end{bmatrix} + \begin{bmatrix} -24.4568 \\ -4.51576 \end{bmatrix} \eta \quad (6.42)$$

Solution of the equations of motion (6.42) using Program CC determines the following reduced-order response transfer functions:

$$\begin{aligned} \frac{w(s)}{\eta(s)} &= \frac{-24.457(s + 59.015)}{(s^2 + 0.893s + 2.704)} \text{ ft/s/rad} \\ \frac{q(s)}{\eta(s)} &= \frac{-4.516(s + 0.455)}{(s^2 + 0.893s + 2.704)} \text{ rad/s/rad (deg/s/deg)} \\ \frac{\alpha(s)}{\eta(s)} &= \frac{-0.077(s + 59.015)}{(s^2 + 0.893s + 2.704)} \text{ rad/rad (deg/deg)} \end{aligned} \quad (6.43)$$

It is important to remember that these transfer functions describe, approximately, the short-term response of those variables which are dominant in short-period motion. The corresponding short-term pitch attitude response transfer function follows since, for small-perturbation motion,

$$\frac{\theta(s)}{\eta(s)} = \frac{1}{s} \frac{q(s)}{\eta(s)} = \frac{-4.516(s + 0.455)}{s(s^2 + 0.893s + 2.704)} \text{ rad/rad (deg/deg)} \quad (6.44)$$

From the pitch rate response transfer function in [equations \(6.43\)](#), it is readily determined that the steady-state pitch rate following a positive unit step elevator input is -0.76 rad/s , which implies that the aircraft pitches continuously until the input is removed. The pitch attitude response transfer function confirms this because, after the short-period transient has damped out, the aircraft behaves like a perfect integrator in pitch. This is indicated by the presence of the s term in the denominator of [equation \(6.44\)](#). In reality, the phugoid dynamics usually prevent this situation unless the input is very large and accompanied by a thrust increase which results in a vertical loop manoeuvre. The model described here would be most inappropriate for the analysis of such large-amplitude motion.

The common denominator of transfer functions (6.43) represents the approximate reduced-order short-period characteristic polynomial, [equation \(6.19\)](#). Thus approximate values of the damping ratio and undamped natural frequency of the short-period mode are easily calculated:

$$\text{Damping ratio } \zeta_s = 0.27$$

$$\text{Undamped natural frequency } \omega_s = 1.64 \text{ rad/s}$$

It will be seen that these values compare very favourably with the exact values given in Example 6.1.

Interpretation of the reduced-order model is probably best illustrated by observing short-term response to an elevator input. The responses to a 1° elevator step input of the variables given in [equations \(6.43\)](#) are shown in [Fig. 6.5](#). Also shown in the same plots are the corresponding responses of the full aircraft model derived from [equation \(6.41\)](#). It is clear that the responses diverge with time, as expected, as no phugoid dynamics are present in the reduced-order model. However, for the first ten seconds or so the comparison is favourable, indicating that the reduced-order model is acceptable for most short-term response studies.

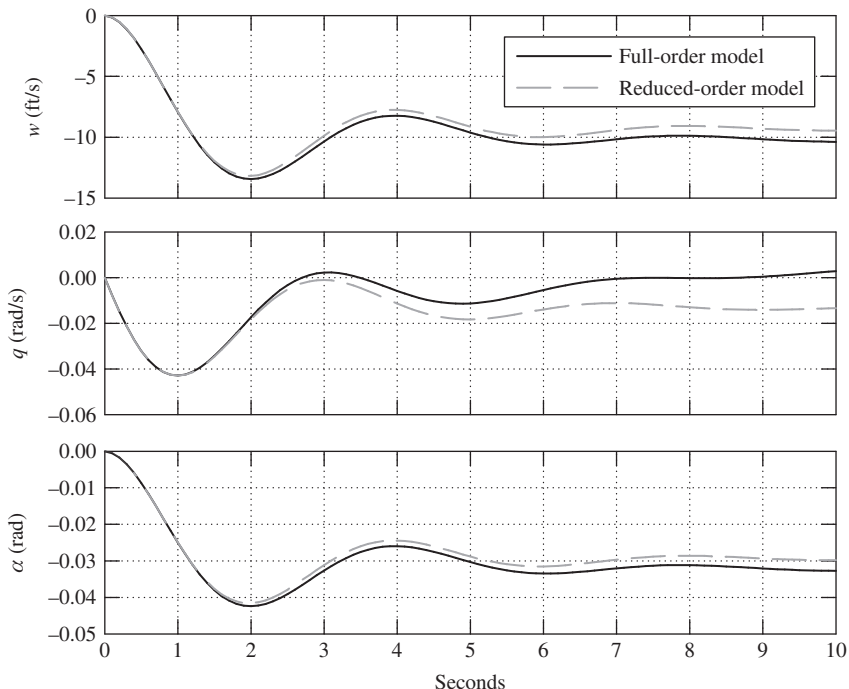


FIGURE 6.5 Reduced-order longitudinal response to a 1° elevator step input.

Turning now to the approximate reduced-order phugoid mode characteristics. From the state equation referred to wind axes, [equation \(6.41\)](#), the required numerical parameters are

$$\begin{aligned}x_u &= -0.04225 \text{ 1/s} \\z_u &= -0.20455 \text{ 1/s} \\m_u &= 0.00003 \text{ rad/ft s} \\U_e \equiv V_0 &= 317.48 \text{ ft/s}\end{aligned}$$

The simple Lanchester model determines that the damping of the phugoid is zero and that the undamped natural frequency is given by [equation \(6.29\)](#). Thus the approximate characteristics of the phugoid mode calculated according to this model are

Damping ratio $\zeta_p = 0$
Undamped natural frequency $\omega_p = 0.143 \text{ rad/s}$

The approximate phugoid mode characteristics determined according to the rather more detailed reduced-order model are given by [equation \(6.36\)](#). Since the chosen flight condition is genuinely subsonic, the derivative m_u is very small indeed, which matches the constraints of the model well. The approximate characteristics of the phugoid mode calculated according to this model are

Damping ratio $\zeta_p = 0.147$
Undamped natural frequency $\omega_p = 0.144 \text{ rad/s}$

Again, comparing these approximate values of the phugoid mode characteristics with the exact values in Example 6.1 indicates good agreement, especially for the undamped natural frequency. Since the phugoid damping ratio is always small (near zero), it is very sensitive to computational rounding errors and to the approximating assumptions, which makes a really good approximate match difficult to achieve. The goodness of the match here is enhanced by the very subsonic flight condition which correlates well with assumptions made in the derivation of the approximate models.

6.4 Frequency response

For the vast majority of flight dynamics investigations, time domain analysis is usually adequate, especially when the subject is the classical unaugmented aeroplane. The principal graphical tool used in time domain analysis is, of course, the time history plot showing the response of the aeroplane to controls or to some external disturbance. However, when the subject aeroplane is an advanced modern aircraft fitted with a flight control system, flight dynamics analysis in the frequency domain can provide additional valuable insight into its behaviour. In recent years frequency domain analysis has made an important contribution to the understanding of the sometimes unconventional handling qualities of aeroplanes whose flying qualities are largely shaped by a flight control system. It is for this reason that a brief review of simple frequency response concepts is considered here. Because frequency response analysis tools are fundamental to classical control

engineering, their description can be found in almost every book on the subject. Very accessible material can be found in [Shinners \(1980\)](#) and [Friedland \(1987\)](#), for example.

Consider the hypothetical situation in which the elevator of an otherwise trimmed aeroplane is operated sinusoidally with constant amplitude k and variable frequency ω . The longitudinal input to the aeroplane may therefore be expressed as

$$\eta(t) = k \sin \omega t \quad (6.45)$$

It is reasonable to expect that each of the output variables describing aircraft motion will respond sinusoidally to the input. However, the amplitudes of the output variables will not necessarily be the same, and they will not necessarily be in phase with one another or with the input. Thus the general expression describing any output response variable may be written as

$$y(t) = K \sin(\omega t + \phi) \quad (6.46)$$

where both output amplitude K and phase shift ϕ are functions of excitation frequency ω . As excitation frequency ω is increased from zero so, initially, at low frequencies, the sinusoidal response is clearly visible in all output variables. As it is increased further, the sinusoidal response starts to diminish in magnitude and eventually becomes imperceptible in the outputs. Simultaneously, phase shift ϕ indicates an increasingly large lag between input and output.

The reason for the observations just given is that, at sufficiently high frequencies, the mass and inertia properties of the aeroplane simply prevent it from responding quickly enough to follow the input. The limiting frequency at which the response commences to diminish rapidly is referred to as the *bandwidth* of the aeroplane with respect to the output variable of interest. A more precise definition of bandwidth is given later. Since aeroplanes respond only to frequencies below the bandwidth frequency, they have the frequency response properties of a *low-pass system*. At exciting frequencies corresponding to the damped natural frequencies of the phugoid and short-period modes, peaks in output magnitude K are seen together, with significant changes in phase shift ϕ . The mode frequencies are described as *resonant*, and the magnitudes of the output parameters K and ϕ at *resonance* are determined by the damping ratios of the modes. The system (or aeroplane) *gain* in any particular response variable is defined as

$$\text{System gain} = \left| \frac{K(\omega)}{k} \right| \quad (6.47)$$

where, in normal control system applications, it is usually assumed that the input and output variables have the same units. This is often not the case in aircraft applications, and care must be exercised in the interpretation of gain.

A number of graphical tools have been developed for the frequency response analysis of linear systems; these include the Nyquist diagram, the Nichols chart, and the Bode diagram. All are intended to simplify analytical procedures, the mathematical calculation of which is tedious without a computer, and all plot input-output gain and phase as functions of frequency. Perhaps the simplest of the graphical tools to use and interpret is the Bode diagram, although the information it is capable of providing is limited. Nevertheless, the Bode diagram is used extensively for flight dynamics analysis, especially in advanced studies of handling qualities.

6.4.1 The Bode diagram

The intention here is not to describe construction of a Bode diagram but to describe its application to the aeroplane and to explain its correct interpretation. For an explanation of Bode diagram construction, the reader should consult a suitable control engineering text, such as either of those referenced in the previous section.

To illustrate the application of the Bode diagram to a typical classical aeroplane, consider the pitch attitude response to elevator transfer function as given by [equation \(6.5\)](#):

$$\frac{\theta(s)}{\eta(s)} = \frac{k_\theta(s + 1/T_{\theta_1})(s + 1/T_{\theta_2})}{(s^2 + 2\zeta_p\omega_p s + \omega_p^2)(s^2 + 2\zeta_s\omega_s s + \omega_s^2)} \quad (6.48)$$

This function is of particular relevance to longitudinal handling studies and has the simplifying advantage that both input and output variables have the same units. In frequency response calculation it is usual to assume a sinusoidal input signal of unit magnitude. Also, it is important that, whenever the response transfer function is negative, which is often the case in aircraft applications, a negative input is assumed which ensures the correct computation of phase. Therefore, in this particular application, since k_θ is usually a negative number, a sinusoidal elevator input of unit magnitude, $\eta(t) = -1 \sin \omega t$ is assumed. The pitch attitude frequency response is calculated by writing $s = j\omega$ in [equation \(6.48\)](#); the right-hand side then becomes a complex number whose magnitude and phase can be evaluated for a suitable range of frequency ω . Since the input magnitude is unity, the *system gain*, [equation \(6.47\)](#), is given simply by the absolute value of the magnitude of the complex number representing the right-hand side of [equation \(6.48\)](#) and is, of course, a function of frequency ω .

Because the calculation of gain and phase involves the products of several complex numbers, it is preferred to work in terms of the logarithm of the complex number representing the transfer function. The total gain and phase then become the simple sums of the gain and phase of each transfer function factor. For example, each factor in parentheses on the right-hand side of [equation \(6.48\)](#) may have its gain and phase characteristics calculated separately as a function of frequency; total gain and phase are then given by summing the contributions from each factor. However, the system gain is now expressed as a logarithmic function of the gain ratio, [equation \(6.47\)](#), defined as

$$\text{Logarithmic Gain} = 20 \log_{10} \left| \frac{K(\omega)}{k} \right| \text{ dB} \quad (6.49)$$

with units of *decibels* (dB). Fortunately, it is no longer necessary to calculate frequency response by hand since many computer software packages, such as MATLAB, have this facility and can also provide the desired graphical output. However, some knowledge of the analytical procedure for obtaining frequency response is, as always, essential so that the computer output may be correctly interpreted.

The Bode diagram comprises the corresponding *gain plot* and *phase plot*. The gain plot shows the logarithmic gain (decibels), plotted against $\log_{10}(\omega)$, and the phase plot shows the phase (degrees), also plotted against $\log_{10}(\omega)$. To facilitate interpretation, the two plots are often superimposed on a common frequency axis. The Bode diagram showing the typical pitch attitude frequency response, as given by transfer function (6.48), is shown in [Fig. 6.6](#).

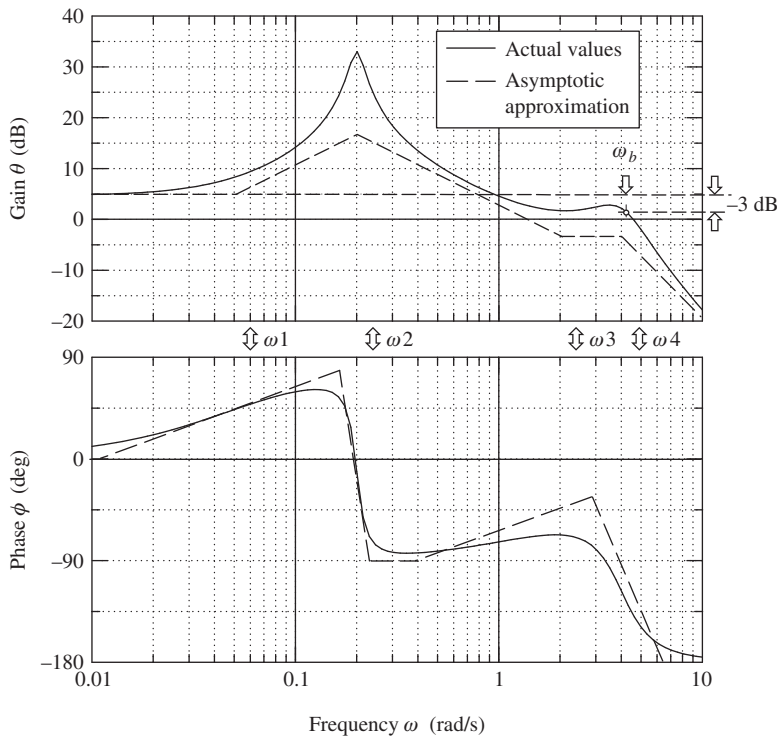


FIGURE 6.6 Bode diagram showing the classical pitch attitude frequency response.

Also shown in Fig. 6.6 are the asymptotic approximations to the actual gain and phase plots as functions of frequency. The asymptotes can be drawn in simply from inspection of the transfer function, equation (6.48), and serve as an aid to interpretation. Quite often the asymptotic approximation is sufficient for the evaluation in hand, thereby dispensing with the need to compute the actual frequency response entirely.

The shape of the gain plot is characterised by the *break frequencies* ω_1 to ω_4 , which determine the locations of the discontinuities in the asymptotic gain plot. Each break frequency is defined by a key frequency parameter in the transfer function:

$$\omega_1 = \frac{1}{T_{\theta 1}} \quad \text{with first-order phase lead } (+45^\circ)$$

$$\omega_2 = \omega_p \quad \text{with second-order phase lag } (-90^\circ)$$

$$\omega_3 = \frac{1}{T_{\theta 2}} \quad \text{with first-order phase lead } (+45^\circ)$$

$$\omega_4 = \omega_s \quad \text{with second-order phase lag } (-90^\circ)$$

Since the transfer function is classical minimum phase, the corresponding phase shift at each break frequency is either a *lead*, if it arises from a numerator term, or a *lag*, if it arises from a denominator term. If, as is often the case in aircraft studies, non-minimum phase terms appear in the transfer function, their frequency response properties are unchanged except that the sign of the phase is reversed. Further, a first-order term gives rise to a total phase shift of 90 deg and a second-order term gives rise to a total phase shift of 180 deg. The characteristic phase response is such that half the total phase shift associated with any particular transfer function factor occurs at the corresponding break frequency. Armed with this limited information, a modest interpretation of the pitch attitude frequency response of the aeroplane is possible. The frequency response of the other motion variables may be dealt with in a similar way.

6.4.2 Interpretation of the Bode diagram

With reference to Fig. 6.6, it is seen that at very low frequencies, $\omega < 0.01$ rad/s, there is no phase shift between the input and output and the gain remains constant—a little below 5 dB in this illustration. In other words, the pitch attitude follows the stick movement more or less precisely. As the input frequency is increased through ω_1 , the pitch response leads the input in phase, the output magnitude increases rapidly, and the aeroplane appears to behave like an *amplifier*. At the phugoid frequency the output reaches a substantial peak, consistent with the low damping, and thereafter the gain drops rapidly, accompanied by a rapid increase in phase lag. As the input frequency is increased further, the gain continues to reduce gently and the phase settles at -90 deg until the influence of break frequency ω_3 comes into play. The reduction in gain is arrested, and the effect of the phase lead may be clearly seen. However, when the input frequency reaches the short-period break frequency, a small peak in gain is seen, consistent with the higher damping ratio, and at higher frequencies the gain continues to reduce steadily. Meanwhile, the phase lag associated with the short-period mode results in a constant total phase lag of -180 deg at higher frequencies.

Once the output-input gain ratio drops below unity, or 0 dB, the aeroplane appears to behave like an *attenuator*. The frequency at which the gain becomes small enough for the magnitude of the output response to become insignificant is called the *bandwidth frequency*, denoted ω_b . There are various definitions of bandwidth, but the one used here is probably the most common and defines bandwidth frequency as the frequency at which the gain first drops to -3 dB below the zero-frequency, or steady-state, gain. The bandwidth frequency is indicated in Fig. 6.6, and it is commonly a little higher than the short-period frequency. A gain of -3 dB corresponds with a gain ratio of $1/\sqrt{2} = 0.707$. Thus, by definition, the gain at the bandwidth frequency is 0.707 times the steady-state gain. Since the pitch attitude bandwidth frequency is close to the short-period frequency, the latter may sometimes be substituted for the bandwidth frequency, which is often good enough for most practical purposes.

The peaks in the gain plot are determined by the characteristics of the stability modes. A very pronounced peak indicates low mode damping and vice versa, an infinite peak corresponding with zero damping. The magnitude of the changes in gain and phase occurring in the vicinity of a peak indicates the significance of the mode in the response variable in question. Fig. 6.6 indicates that the magnitude of the phugoid is much greater than the magnitude of the short-period mode in the pitch response of the aeroplane. This is in fact confirmed by response time histories and inspection of the corresponding eigenvectors.

In the classical application of the Bode diagram, as used by the control engineer, inspection of the gain and phase properties in the vicinity of the bandwidth frequency enables conclusions to be made about the stability of the system. Typically, stability is quantified in terms of *gain margin* and *phase margin*. However, such evaluations are only appropriate when the system transfer function is *minimum phase*. Since aircraft transfer functions that are non-minimum phase are frequently encountered, and many also have the added complication that they are negative, it is not usual for aircraft stability to be assessed in the Bode diagram. It is worth noting that, for aircraft augmented with flight control systems, the behaviour of the phase plot in the vicinity of the bandwidth frequency is now known to be linked to the susceptibility of the aircraft to *pilot-induced oscillations*, a particularly nasty handling deficiency.

The foregoing summary interpretation of frequency response assumes a sinusoidal elevator input to the aircraft. Clearly, this is never likely to occur as a result of normal pilot action, but normal pilot actions may be interpreted to comprise a mix of many different frequency components. For example, in gentle manoeuvring the frequency content of the input is generally low whilst in aggressive or high-workload situations the frequency content is higher and may even exceed the bandwidth of the aeroplane. In such a limiting condition the pilot is certainly aware that the aeroplane cannot follow his demands quickly enough and, depending in detail on the gain and phase response properties of the aeroplane, he may well encounter hazardous handling problems. For this reason, bandwidth is a measure of the *quickness of response* achievable in a given aeroplane. As a general rule, it is desirable that flight control system designers seek the highest-response bandwidth consistent with the dynamic capabilities of the airframe.

EXAMPLE 6.3

The longitudinal frequency response of the A-7A Corsair II aircraft is evaluated for the same flight condition as in Examples 6.1 and 6.2. However, the longitudinal response transfer functions used for the evaluations are referred to wind axes and were obtained in the solution of the full-order state [equation \(6.41\)](#). The transfer functions of primary interest are

$$\begin{aligned}\frac{u(s)}{\eta(s)} &= \frac{0.00381(s + 0.214)(s + 135.93)(s + 598.3)}{(s^2 + 0.033s + 0.02)(s^2 + 0.902s + 2.666)} \text{ ft/s/rad} \\ \frac{\theta(s)}{\eta(s)} &= \frac{-4.516(s - 0.008)(s + 0.506)}{(s^2 + 0.033s + 0.02)(s^2 + 0.902s + 2.666)} \text{ rad/rad} \\ \frac{\alpha(s)}{\eta(s)} &= \frac{-0.077(s^2 + 0.042s + 0.02)(s + 59.016)}{(s^2 + 0.033s + 0.02)(s^2 + 0.902s + 2.666)} \text{ rad/rad}\end{aligned}\quad (6.50)$$

It will be noticed that the values of the various numerator terms in the velocity and incidence transfer functions differ significantly from the values in the corresponding transfer functions in Example 6.1, [equations \(6.8\)](#). This is due to the different reference axes used and to the fact that the angular difference between body and wind axes is a significant body incidence angle of 13.3 deg. Such a large angle is consistent with the very low speed flight condition. The frequency response of each transfer function was calculated with the aid of Program CC, and the Bode

diagrams are shown, in Figs. 6.7 through 6.9 respectively. Interpretation of the diagrams for the three variables is straightforward and follows the general interpretation discussed earlier. However, important or significant differences are commented on as follows.

The frequency response of axial velocity u to elevator input η is shown in Fig. 6.7, and it is clear, as might be expected, that it is dominated by the phugoid. The very large low-frequency gain values are due entirely to the transfer function units, which are in ft/s/rad, and a unit radian elevator input is of course unrealistically large! The peak gain of 75 dB at the phugoid frequency corresponds with a gain ratio of approximately 5600 ft/s/rad. However, since the aircraft model is linear, this may be interpreted equivalently as approximately 98 ft/s/deg, which is much easier to appreciate physically. Since the gain drops away rapidly as the frequency increases beyond the phugoid frequency, the velocity bandwidth frequency is only a little higher than the phugoid frequency. This accords well with practical observation: Velocity perturbations at frequencies in the vicinity of the short-period mode are usually insignificantly small. The phase plot indicates that there is no appreciable phase shift between input and output until the frequency exceeds the

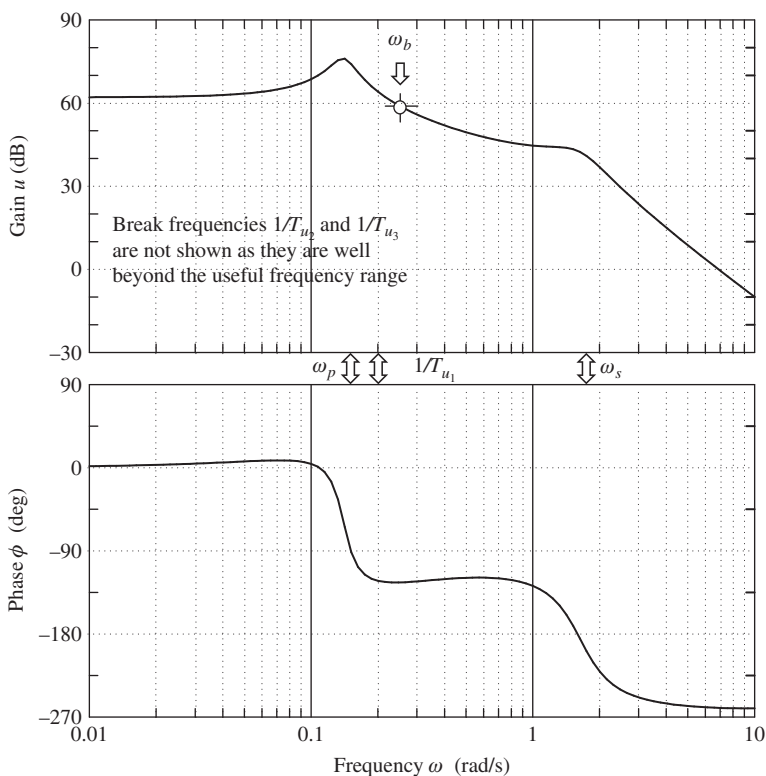


FIGURE 6.7 A-7A velocity frequency response.

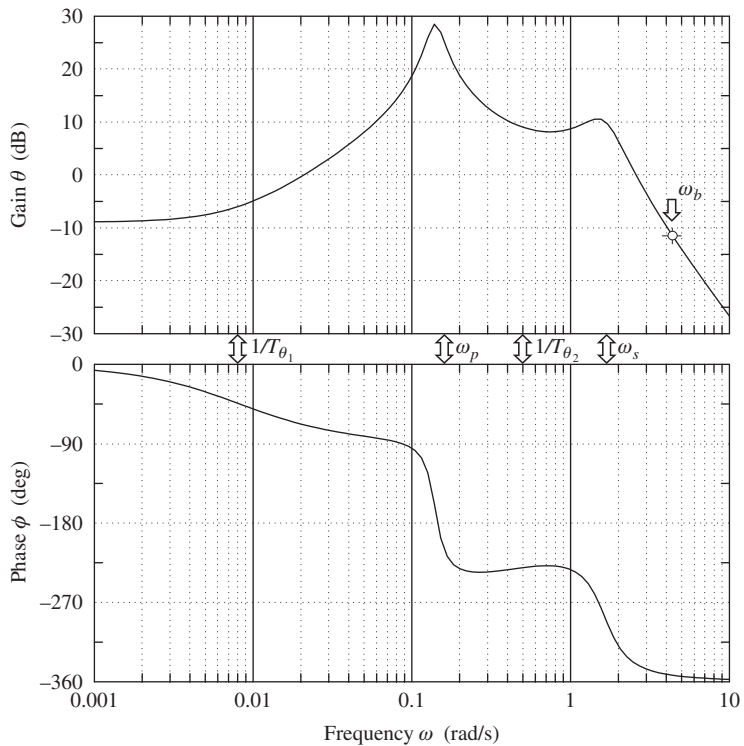


FIGURE 6.8 A-7A pitch attitude frequency response.

phugoid frequency, when there is a rapid increase in phase lag. This means that, for all practical purposes, speed changes demanded by the pilot follow the stick in the usable frequency band.

The pitch attitude θ frequency response to elevator input η is shown in Fig. 6.8. General interpretation of this figure follows the discussion of Fig. 6.6 and is not repeated here. However, there are some significant differences which must not be overlooked. These differences are due to the fact that the transfer function is non-minimum phase, a consequence of selecting a very-low-speed flight condition for the example. Referring to equations (6.50), this means that the numerator zero $1/T_{\theta_1}$ is negative, and the reasons for this are discussed in Example 6.1.

The non-minimum phase effects do not influence the gain plot in any significant way, so its interpretation is quite straightforward. However, the effect of the nonminimum phase numerator zero is to introduce phase lag at very low frequencies rather than the usual phase lead. It is likely that, in manoeuvring at this flight condition, the pilot is aware of the pitch attitude lag in response to his stick input.

The body incidence α frequency response to elevator input η is shown in Fig. 6.9, and it is clear, as might be expected, that this is dominated by the short-period mode. For all practical purposes,

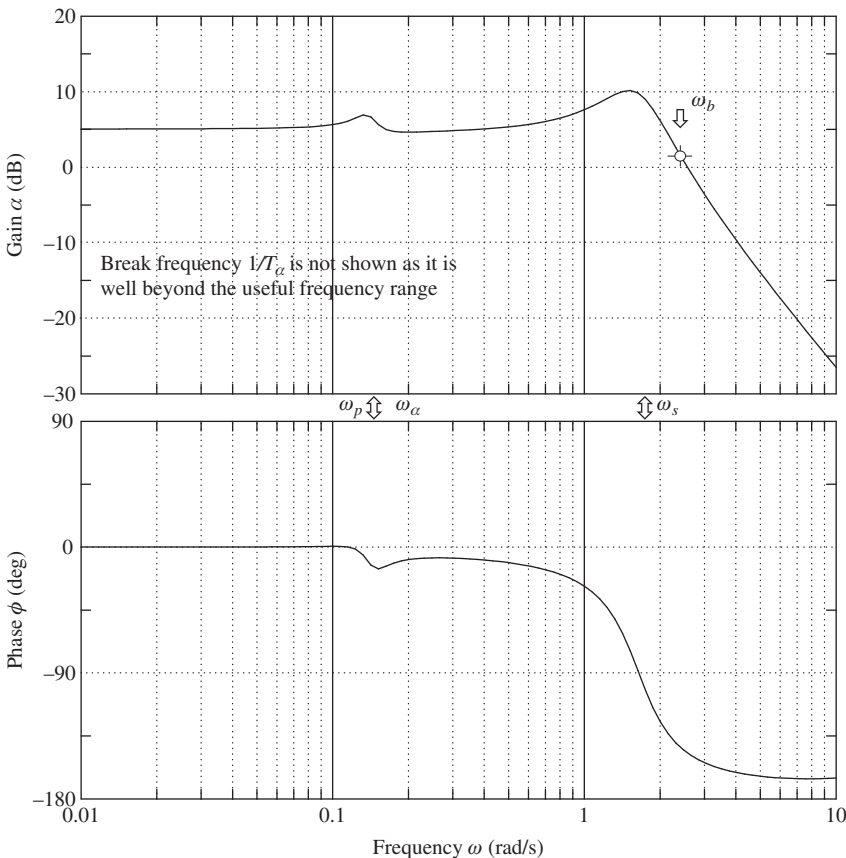


FIGURE 6.9 A-7A body incidence frequency response.

the influence of the phugoid on both gain and phase frequency responses is insignificant, which may be confirmed by reference to the appropriate transfer function in [equations \(6.50\)](#). There it is seen that the second-order numerator term very nearly cancels the phugoid term in the denominator. This is an important observation since it is quite usual to cancel approximately equal numerator and denominator terms in any response transfer function to simplify it.

Simplified transfer functions often provide adequate response models in both the time and frequency domains, and can be extremely useful for explaining and interpreting aircraft dynamic behaviour. In modern control parlance the phugoid dynamics are said to be *not observable* in this illustration. The frequency response in both gain and phase is more or less *flat* at frequencies up to the short-period frequency, or for most of the usable frequency range. In practical terms, this means that incidence follows the stick at constant gain and without appreciable phase lag, obviously a desirable state of affairs.

6.5 Flying and handling qualities

The longitudinal stability modes play a fundamental role in determining the longitudinal flying and handling qualities of an aircraft and it is essential that their characteristics must be “correct” if the aircraft is to be flown by a human pilot. A simplistic view of the human pilot suggests that he behaves like an adaptive dynamic system and will adapt his dynamics to harmonise with those of the controlled vehicle. Since his dynamics interact and couple with those of the aircraft, he will adapt, within human limits, to produce the best *closed-loop* system dynamics compatible with the piloting task. His adaptability enables him to cope with an aircraft with less than desirable flying qualities.

However, the problems of coupling between incompatible dynamic systems can be disastrous no stop and it is this latter aspect of the piloting task that has attracted much attention in recent years. Every time the aircraft is disturbed in response to control commands, the stability modes are excited and it is not difficult to appreciate why their characteristics are so important. Similarly, the stability modes are equally important in determining *ride quality* when the main concern is response to atmospheric disturbances. In military combat aircraft, ride quality determines the effectiveness of the airframe as a weapons platform; in the civil transport aircraft, it determines the comfort of passengers.

In general, it is essential that the short-period mode, which has a natural frequency close to human pilot natural frequency, is adequately damped. Otherwise, dynamic coupling with the pilot may occur under certain conditions, leading to severe, or even catastrophic, handling problems. On the other hand, as the phugoid mode is much lower in frequency, its impact on the piloting task is much less demanding. The average human pilot can easily control the aircraft even when the phugoid is mildly unstable. The phugoid mode can, typically, manifest itself as a minor trimming problem when poorly damped. Although not in itself hazardous, this can lead to increased pilot workload, and for this reason it is desirable to ensure adequate phugoid damping. It is also important that the natural frequencies of the stability modes should be well separated in order to avoid interaction, or coupling, between the modes. Mode coupling may give rise to unusual handling characteristics and is generally regarded as an undesirable feature in longitudinal dynamics. The subject of aircraft handling qualities is discussed in rather more detail in Chapter 10.

6.6 Mode excitation

Because the longitudinal stability modes are usually well separated in frequency, it is possible to excite them more or less independently for purposes of demonstration or measurement. Indeed, it is a general flying qualities requirement that the modes be well separated in frequency to avoid handling problems arising from dynamic mode coupling. The modes may be excited selectively by a sympathetic elevator input to the trimmed aircraft. The methods developed for in-flight mode excitation reflect an intimate understanding of the dynamics involved and are generally easily adapted to the analytical environment. Because the longitudinal modes are usually well separated in frequency, the form of the input disturbance is not, in practice, very critical. However, some consistency in the flight test analytical procedures adopted is desirable if meaningful comparative studies are to be made.

The short-period pitching oscillation may be excited by applying a short-duration disturbance in pitch to the trimmed aircraft. This is best achieved with an elevator pulse with a duration of a second or less. Analytically, this is adequately approximated by a unit impulse applied to the elevator. The essential feature of the disturbance is that it must be sufficiently short so as not to significantly excite the phugoid. However, as the phugoid damping is usually very low it is almost impossible not to excite the phugoid at the same time but, it does not usually develop fast enough to obscure observation of the short-period mode.

An example of a short-period response recorded during a flight test exercise in a Handley Page Jetstream aircraft is shown in Fig. 6.10. In fact, two excitations are shown, the first in the nose-up

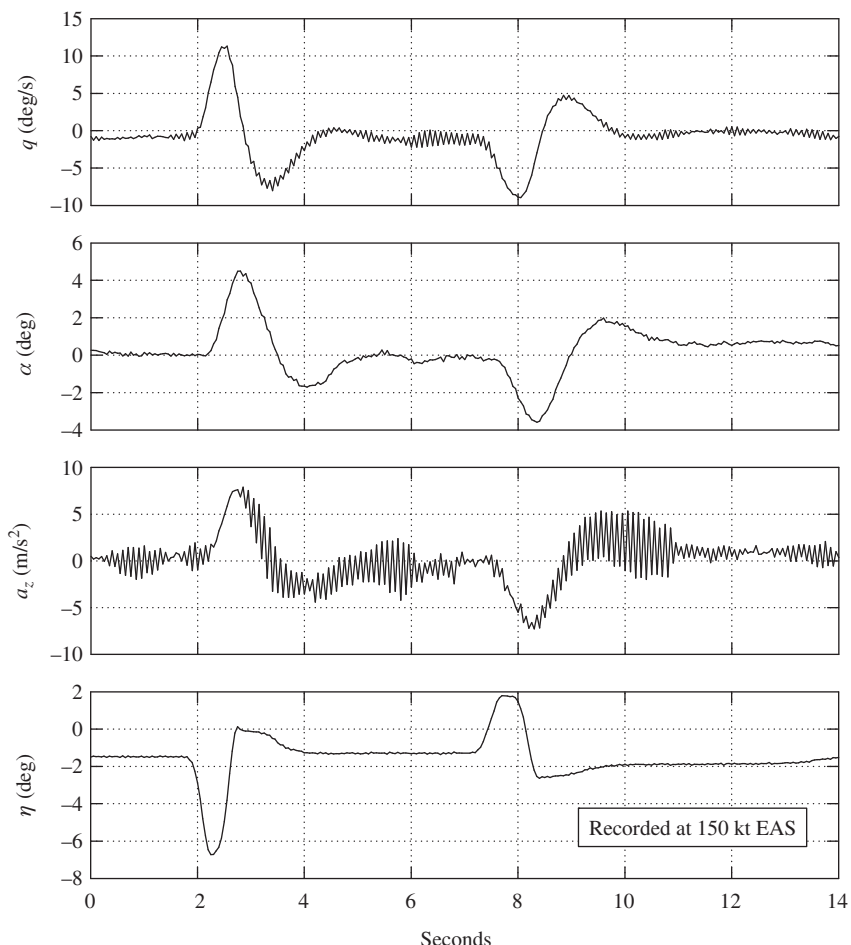


FIGURE 6.10 Flight recording of the short-period pitching oscillation.

sense and the second in the nose-down sense. The pilot input “impulse” is clearly visible and represents his best attempt at achieving a clean impulse-like input; some practice is required before consistently good results are obtained. Immediately following the input the pilot released the controls to obtain the controls-free dynamic response, which explains why the elevator angle does not recover its equilibrium trim value until the short-period transient has settled. During this short elevator free period, its motion is driven by oscillatory aerodynamic loading and is also coloured by the control circuit dynamics, which can be noticeably intrusive. Otherwise the response is typical of a well damped aeroplane.

The phugoid mode may be excited by applying a small speed disturbance to the aircraft in trimmed flight. This is best achieved by applying a small step input to the elevator which causes the aircraft to fly up or down according to the sign of the input. If the power is left at its trimmed setting, the speed will decrease or increase accordingly. When the speed has diverged from its steady trimmed value by about 5%, the elevator is returned to its trim setting. This provides the disturbance, and a stable aircraft will then execute a phugoid oscillation as it recovers its trim equilibrium. Analytically, the input is equivalent to an elevator pulse of several seconds’ duration. The magnitude and length of the pulse would normally be established by trial and error since its effect is very aircraft dependent. However, it should be remembered that for proper interpretation of the resulting response, the disturbance should be small in magnitude since a small-perturbation model is implied.

An example of a phugoid response recorded during a flight test exercise in a Handley Page Jetstream aircraft is shown in Fig. 6.11. The pilot input “pulse” is clearly visible and, as for the short-period mode, some practice is required before consistently good results are obtained. Again, the controls are released following the input to obtain the controls-free dynamic response, and the subsequent elevator motion is caused by the sinusoidal aerodynamic loading on the surface itself. The leading and trailing edge “steps” of the input elevator pulse may excite the short-period mode, but the short-period mode transient normally decays to zero well before the phugoid has properly developed and therefore would not obscure the observation of interest.

It is clear from inspection of Fig. 6.11 that the phugoid damping is significantly higher than might be expected from the previous discussion of mode characteristics. What is in fact shown is the aerodynamic, or basic airframe, phugoid modified by the inseparable effects of power. The Astazou engines of the Jetstream are governed to run at constant rpm, and thrust changes are achieved by varying the propeller blade pitch. Thus, as the aircraft flies the sinusoidal flight path during a phugoid disturbance, the sinusoidal propeller loading causes the engine to automatically adjust its power to maintain constant propeller rpm. This very effectively increases the apparent phugoid damping. It is possible to operate the aircraft at a constant power condition when the “power damping” effect is suppressed. Under these circumstances, the aerodynamic phugoid is found to be much less stable, as predicted by the simple theoretical model, and at some flight conditions is unstable.

The above flight recording of the longitudinal stability modes illustrates the *controls-free* dynamic stability characteristics. The same exercise could of course be repeated with the controls held fixed following the disturbing input; then the *controls-fixed* dynamic stability characteristics would be observed. In general, the differences between responses would be small and not too significant. Now controls-free dynamic response is only possible in aeroplanes with reversible controls, which includes most small classical aeroplanes. Virtually all larger modern aircraft have

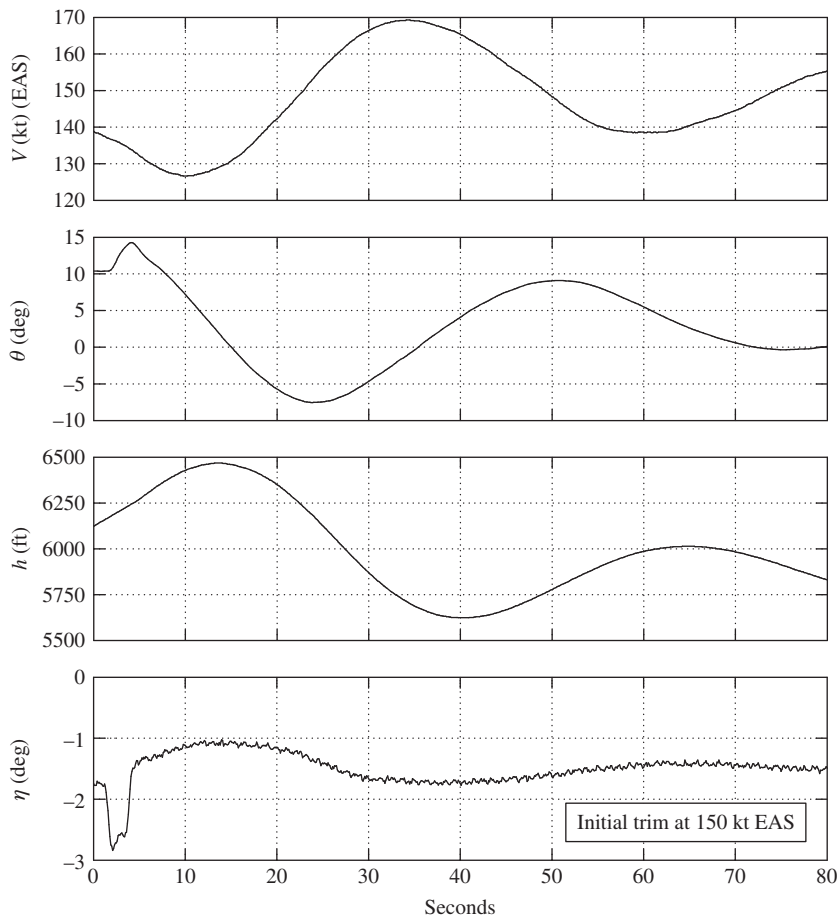


FIGURE 6.11 Flight recording of the phugoid.

powered controls, driven by electronic flight control systems, which are effectively irreversible. This means that such aircraft are only capable of controls-fixed dynamic response. For this reason, most current theoretical modelling and analysis is concerned with controls-fixed dynamics only, as is the case throughout this book. However, a discussion of the differences between controls-fixed and controls-free aeroplane dynamics may be found in Hancock (1995).

When it is required to analyse the dynamics of a single mode in isolation, the best approach is to emulate flight test practice as far as that is possible. It is necessary to choose the most appropriate transfer functions to show the dominant response variables in the mode of interest. For example, as illustrated in Figures 6.10 and 6.11, the short-period mode is best observed in the dominant response variables q and $w(\alpha)$ whereas the phugoid is best observed in its dominant response

variables u , h , and θ . It is necessary to apply a control input disturbance sympathetic to the mode dynamics, and it is also necessary to observe the response for an appropriate period of time. For example, Fig. 6.1 shows both longitudinal modes, but the time scale of the illustration reveals the phugoid mode in much greater detail than the short-period mode. Whereas, the time scale of Fig. 6.5 was chosen to reveal the short-period mode in detail since that is the mode of interest. The form of the control input is not usually difficult to arrange in analytical work because most software packages have built-in impulse, step, and pulse functions, whilst more esoteric functions can usually be programmed by the user. This kind of informed approach to analysis is required if the best possible visualisation of the longitudinal modes and their associated dynamics is to be obtained.

References

- Friedland, B. (1987). *Control system design*. New York: McGraw-Hill.
 Hancock, G. J. (1995). *An introduction to the flight dynamics of rigid aeroplanes*. Hemel Hempstead: Ellis Horwood Ltd.
 Lanchester, F. W. (1908). *Aerodonetics*. London: Constable and Co. Ltd.
 Shinners, S. M. (1980). *Modern control system theory and application*. Boston: Addison-Wesley.
 Teper, G. L. (1969). *Aircraft stability and control data*. Systems Technology, Inc., STI Technical Report 176-1. NASA Contractor Report, National Aeronautics and Space Administration, Washington D.C. 20546.

PROBLEMS

- 6.1** A tailless aeroplane of 9072 kg mass has an aspect ratio 1 delta wing of area 37 m². The longitudinal short-period motion of the aeroplane is described by the characteristic quadratic

$$\lambda^2 + B\lambda + C = 0$$

where

$$B = \frac{1}{2} \left(\frac{dC_L}{d\alpha} \right) \cos^2 \alpha$$

and

$$C = -\frac{1}{2} \left(\frac{\mu_1}{i_y} \right) \left(\frac{dC_m}{d\alpha} \right) \cos \alpha$$

α is the wing incidence, $\mu_1 = m/\frac{1}{2}\rho S \bar{c}$ is the longitudinal relative density parameter, and $i_y = I_y/m \bar{c}^2$ is the dimensionless moment of inertia in pitch. The aeroplane's moment of inertia in pitch is 1.356×10^5 kg/m². The variation of C_L and C_m with incidence $\alpha > 0$ is non-linear for the aspect ratio 1 delta wing:

$$C_L = \frac{1}{2} \pi \alpha + 2\alpha^2$$

$$C_m = C_{m_0} - 0.025\pi\alpha - 0.1\alpha^2$$

Describe and compare the short-period motions when the aeroplane is flying straight and level at 152 m/s at sea level and at 35,000 ft.

$$\rho_0 = 1.225 \text{ kg/m}^3 \text{ at sea level; } \rho/\rho_0 = 0.310 \text{ at 35,000 ft; characteristic time } \sigma = m/\frac{1}{2}\rho V_0 S. \quad (\text{CU 1983})$$

- 6.2 (a) List the characteristics of the longitudinal phugoid stability mode.
 (b) List the characteristics of the longitudinal short-period pitching stability mode.
 (c) The transfer function for the unaugmented McDonnell F-4C Phantom describing the pitch attitude response to elevator when flying at Mach 1.2 at an altitude of 35,000 ft is given by

$$\frac{\theta(s)}{\eta(s)} = \frac{-20.6(s + 0.013)(s + 0.62)}{(s^2 + 0.017s + 0.002)(s^2 + 1.74s + 29.49)} \text{ rad/rad}$$

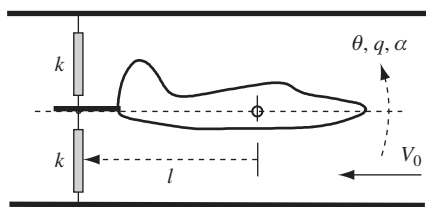
Write down the longitudinal characteristic equation and state whether the aeroplane is stable, or not.

- (d) What are the numerical parameters describing the longitudinal stability modes of the McDonnell F-4C Phantom?

(CU 1999)

- 6.3 Describe the longitudinal short-period pitching oscillation. On what parameters do its characteristics depend?

A model aircraft is mounted in a wind tunnel such that it is free to pitch about an axis through its *cg* as shown. The model is restrained by two springs attached at a point on a fuselage aft extension which is at a distance $l = 0.5 \text{ m}$ from the *cg*. The model has wing span $b = 0.8 \text{ m}$, mean aerodynamic chord $\bar{c} = 0.15 \text{ m}$ and the air density may be taken as $\rho = 1.225 \text{ kg/m}^3$.



With the wind off, the model is displaced in pitch and released. The frequency of the resulting oscillation is 10 rad/s, and the damping ratio is 0.1. The experiment is repeated with a wind velocity $V_0 = 30 \text{ m/s}$, the frequency is now found to be 12 rad/s, and the damping ratio is 0.3. Given that the spring stiffness $k = 16 \text{ N/m}$, calculate the moment of inertia in pitch and the values for the dimensionless stability derivatives M_q and M_w . It may be assumed that the influence of the derivative $M_{\dot{w}}$ is negligible. State all assumptions made.

(CU 1987)

- 6.4** (a) Show that the period of the phugoid is given approximately by $T_p = \sqrt{2\pi} \frac{V_0}{g}$, and state all assumptions used during the derivation.
 (b) State which aerodynamic parameters introduce damping into a phugoid, and discuss how varying forward speed whilst on approach to landing may influence phugoid characteristics.

(LU 2001)

- 6.5** (a) Using a simple physical model, show that the short-period pitching oscillation can be approximated by

$$I_y \ddot{\theta} + \frac{1}{2} \rho V_0^2 a_1 S_T l_T^2 \dot{\theta} - \frac{1}{2} \rho V_0^2 S \bar{c} \frac{dC_m}{d\alpha} \theta = 0$$

- (b) The aircraft described here is flying at sea level at 90 m/s. Determine the centre of gravity location at which the short-period pitching oscillation ceases to be oscillatory.

Wing lift curve slope = 5.7 1/rad

Tailplane lift curve slope = 3.7 1/rad

Horizontal tail arm = 6 m

Tailplane area = 5 m²

$d\varepsilon/d\alpha = 0.30$

$I_y = 40,000 \text{ kg/m}^2$

Wing area = 30 m²

Mean aerodynamic chord = 1.8 m

Aerodynamic centre = 0.18 \bar{c}

Hint: Modify the equation in part (a) to include tailplane lag effects.

- (c) Determine the period of the short-period pitching oscillation if the *cg* location is moved 0.2 \bar{c} forward of the position calculated in part (b).

(LU 2001)

- 6.6** For a conventional aircraft on approach to landing, discuss how the aircraft's aerodynamics may influence longitudinal stability.

(LU 2002)

- 6.7** Determine the time to half-amplitude and the period of the short-period pitching oscillation. Assume that the short-period pitching oscillation can be approximated by

$$I_y \ddot{\theta} - \frac{\partial M}{\partial q} \dot{\theta} - \frac{\partial M}{\partial w} V \theta = 0 \text{ and } M_w = \partial C_m / \partial \alpha$$

(LU 2003)